

Resonant Plasmonic Nanoslits Enable in Vitro Observation of Single-Monolayer Collagen-Peptide Dynamics

Rostyslav Semenyshyn,^{†,‡} Mario Hentschel,^{†,‡} Christian Huck,[§] Jochen Vogt,[§] Felix Weiher,[†] Harald Giessen,^{†,‡} and Frank Neubrech^{*,†,§}

[†]4th Physics Institute and Research Center SCoPE, University of Stuttgart, Pfaffenwaldring 57, 70569 Stuttgart, Germany

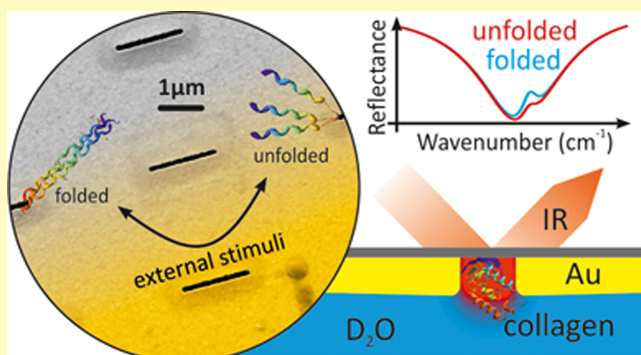
[‡]Center for Integrated Quantum Science and Technology, IQST, Pfaffenwaldring 57, 70569 Stuttgart, Germany

[§]Kirchhoff Institute for Physics, University of Heidelberg, Im Neuenheimer Feld 227, 69120 Heidelberg, Germany

Supporting Information

ABSTRACT: Proteins perform a variety of essential functions in living cells and thus are of critical interest for drug delivery as well as disease biomarkers. The different functions are derived from a hugely diverse set of structures, fueling interest in their conformational states. Surface-enhanced infrared absorption spectroscopy has been utilized to detect and discriminate protein monomers. As an important step forward, we are investigating collagen peptides consisting of a triple helix. While they constitute the main structural building blocks in many complex proteins, they are also a perfect model system for the complex proteins relevant in biological systems. Their complex spectroscopic information as well as the overall small size present a significant challenge for their detection and discrimination. Using resonant plasmonic nanoslits, which are known to show larger specificity compared to nanoantennas, we overcome this challenge. We perform in vitro surface-enhanced absorption spectroscopy studies and track the conformational changes of these collagen peptides under two different external stimuli, which are temperature and chemical surroundings. Modeling the coupling between the amide I vibrational modes and the plasmonic resonance, we can extract the conformational state of the collages and thus monitor the folding and unfolding dynamics of even a single monolayer. This leads to new prospects in studies of single layers of proteins and their folding behavior in minute amounts in a living environment.

KEYWORDS: plasmonics, surface-enhanced infrared absorption spectroscopy, collagen peptides, conformational changes, biosensing



Proteins are large, complex molecules performing many critical functions in the body. They do most of the work in living cells and are required for the structure, function, and regulation of body tissues and organs. Proteins are long chains of amino acids,^{1,2} whose linear sequences are termed the primary structure of the protein.³ Hydrogen bonding between amino groups and carboxyl groups in the neighboring regions of the protein chain lead to a distinct folding behavior.⁴ These stable folding patterns are the so-called secondary structures of a protein. The final shape is typically the most energetically favorable one.⁵ During the folding process, the proteins might undergo a variety of conformations before reaching their final form, which is unique. Furthermore, chemical forces between a protein and its immediate environment contribute to protein shape and stability. Consequently, some misfolded proteins are believed to cause systematic or neurodegenerative diseases.^{6,7}

A number of different techniques allow for the examination of protein secondary structure (e.g., nuclear magnetic resonance (NMR) spectroscopy or atomic force microscopy).^{2,8–15} However, to detect the structural changes for

small amounts, such as on a monolayer scale, using those tools is extremely difficult or even impossible, as they require large amounts of analyte or cannot be performed in vitro, that is, in aqueous surroundings. In contrast, infrared (IR) vibrational spectroscopy is a powerful tool for the identification of the structural conformation of molecules, which is in principle scalable.^{16–18} The molecular bonds result in a unique optical response due to vibrational excitations at characteristic frequencies, causing distinct so-called vibrational fingerprints. Monitoring the spectral response of an analyte enables a label-free optical detection of molecular species. More importantly, the optical response is modified whenever a certain molecular structure changes due to an external stimulus.^{19–23} However, similarly to the other mentioned techniques, conventional vibrational spectroscopy requires large amounts of molecules in order to detect the molecular conformation due to the

Received: February 22, 2019

Accepted: May 28, 2019

Published: May 28, 2019

relatively small infrared absorption cross sections of the molecules. Resonant plasmonic nanoparticles can overcome this limitation and enable vibrational spectroscopy at low concentrations. Namely, surface-enhanced infrared absorption (SEIRA) spectroscopy utilizes the strong near-fields of the metallic nanostructures to enhance the infrared vibrational modes of molecules.^{24–26} One can also reach much higher sensitivity with resonant SEIRA,^{26–32} where the frequency of the plasmonic mode and the molecular vibration are matched. It enables the detection of minute amounts of molecules on the plasmonic structures down to attomolar sensitivity.^{24,33} The only difficulty lies with sample preparation, as the molecules need to be positioned in the plasmonic near-fields. However, the required surface modifications are in fact well under control, and thus, SEIRA allows for in vitro probing of molecular monolayers.

Nanoantenna arrays were already successfully used for biosensing^{11,31,34–37} in air as well as aqueous surroundings,^{38–41} even in real-time,⁴² demonstrating the reliable detection of monolayers of proteins. In these studies, folding of monomers, that is, single chains of amino acids, under chemical stimulus has been detected and monitored. Importantly, biologically relevant proteins and peptides are in fact much larger or more complex than the monomers studied to date and are commonly composed of several individual monomers. Collagens are a particularly interesting system, as they are so-called trimers, consisting of a triple helix of peptides with polyproline helical structure. *Such collagens are in fact structural building blocks in many complex proteins and thus constitute an ideal model system for the more complex and biologically relevant systems.*

In this contribution, we demonstrate in vitro monitoring of structural changes of collagen-like molecules utilizing resonant plasmonic nanoslits as a sensing platform based on surface-enhanced infrared absorption spectroscopy. These results go beyond the current state-of-the-art for two reasons: First, we study more complex molecular entities, which show a diverse and intricate spectral response. While this is an important step on the quest for improved molecular recognition for biologically relevant entities, it also requires better sensitivity, as the collagens are in fact small molecules exhibiting comparably small vibrational signal strengths. These expected small signals require a modeling of the coupling between the plasmonic resonance and the molecular vibration in order to extract the conformational change from the spectral response. Second, we are reporting the use of plasmonic nanoslits as a SEIRA platform, which is known for its improved specificity compared to solid nanoantennas together with these more complex biomolecules. Figure 1 illustrates the basic idea of our experimental study. Standard Fourier transform (FT) infrared spectroscopy is performed to probe the optical response of resonant plasmonic nanoslits, in inverse reflection geometry. According to Babinet's principle,^{43,44} the inverse nanostructures also feature plasmonic resonances and, as it was shown, even provide a higher average SEIRA signal.⁴⁵ Furthermore, nanoslits exhibit a smaller resonance shift for a changing effective refractive index, which is unavoidable during temperature changes of the sensing solution. Thus, in order to perform in vitro measurements, nanostructures are immersed in the aqueous surroundings and are covered by a monolayer of capped collagen peptides,⁴⁶ which are about 5 kDa in weight and can be used as a folding model for minicollagen proteins (Figure S1 in the Supporting Information). In the unfolded

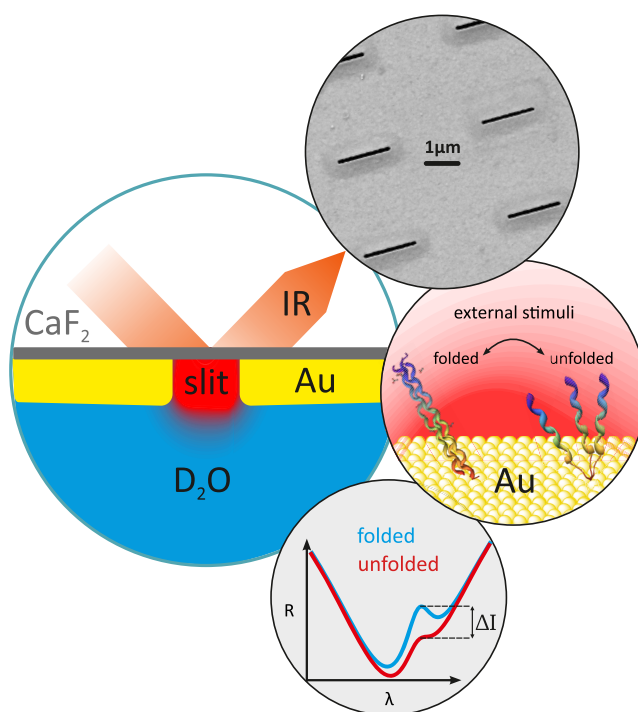


Figure 1. A monolayer of collagen-peptide 3x(PUG)₅ is immobilized on the gold (Au) surface of nanoslit arrays. The amide vibration of 3x(PUG)₅ is enhanced if the plasmon is resonantly matched to the molecular vibration. We apply an external stimulus, which leads to structural changes of the molecules, resulting in different intensities of the amide vibration, allowing optical tracking of the conformational changes of molecules. The optical response is measured in inverse reflection geometry. The SEM image depicts an exemplary nanoslit array; the scale bar is 1 μm .

state, the distinct single chains of the molecule exhibit only partial polyproline type secondary structures. A cooperative folding behavior leads to collagen's typical triple-helical structure in the folded state. To observe folding of triple helices, the monitoring of the intrahelical vibrations is required,⁴⁷ and thus, high SEIRA signal is necessary. The conformational changes of collagen peptides are induced by two different external stimuli, namely, a surfactant as well as temperature change. Monitoring the amide vibration, which is characteristic for bonded helices, we are able to detect the secondary structure of the molecules and its dependence on the surrounding properties.

EXPERIMENTAL RESULTS AND DISCUSSION

In order to perform surface-enhanced infrared absorption spectroscopy, we need to place the molecules into the so-called "hot spots" of the nanostructure. As we are going to utilize nanoslits, the collagen peptides should be located inside the slits, where the near-field is maximum.⁴⁵ The most straightforward option is to bind the peptides to the gold surface itself with standard gold–thiol chemistry. The peptides will therefore also be present inside the slits, as they can cover the side walls. Instead of a sequential assembly as presented in other work,^{48,41} we utilize specially synthesized capped collagen peptides with a thiol group at the end (Figure S1 in the Supporting Information).⁴⁶ This allows us to directly dress the gold surface with a self-assembled monolayer of collagen peptides.

To start with the folding studies, we utilize a tailored reflection flow cell (Figure S2 in the Supporting Information), which allows for measuring the nanostructures in an aqueous environment in inverse reflection geometry. The nanoslit fabrication consists of a standard electron beam lithography (EBL) process and subsequent argon-ion milling.⁴⁵ We used a patterned poly(methyl methacrylate) (PMMA) layer as an etching mask on top of a 50 nm thin gold mirror and thus were able to produce nanoslit arrays ($200 \times 200 \mu\text{m}$) of different sizes. We varied the slits length between 1.4 and $2.1 \mu\text{m}$ with an optimal constant lateral spacing of $3 \mu\text{m}$ in the x -direction (along the long slit axis) and $2.5 \mu\text{m}$ in the y -direction (along the short slit axis) and a slit width of 70 nm (Figure S3 in the Supporting Information). As an adhesion layer on CaF_2 substrate, we used titanium because of its chemical stability. Here, one should mention that H_2O exhibits vibrational signals in the amide I spectral range, and thus, we perform the measurements in D_2O -based solutions, which vibrate at lower energies.⁴¹ Finally, to study the structural changes of the collagen-peptide monolayer, we cover the sample with molecules by immersing the slits into $5 \mu\text{M}$ D_2O -based solution of collagen peptides functionalized with thiol bonds for 24 h.

Figure 2a depicts the reflectance of $1.7 \mu\text{m}$ long nanoslits being immersed in D_2O before (dark green) and after (dark red) functionalization. First of all, a red shift of the plasmon resonance frequency is observed after molecules covered the sample. This is expected, as collagens adsorbed on the gold surface slightly increase the effective refractive index. As we are more interested in the spectral region of the amide vibration (vertical dashed line), we zoom-in on the optical response at this frequency, shown in Figure 2b. As one can see, a spectral feature is imprinted onto the reflectance spectrum of functionalized slits, which is not observed for the bare sample (upper panel). At first sight, the signal appears very small. However, such a weak signal is in fact expected due to the small size of the molecules and thus the small number of $\text{C}=\text{O}$ stretch vibrations. As we want to observe the changes of amide vibration, we therefore require another data representation. To accomplish this, we plot the first derivative of the optical response (lower panel). Indeed, the signal now becomes clearly visible exactly at the frequency of collagen-peptides' amide vibration, which proves that a thin monolayer of molecules covers the gold surface and allows us to track the changes of spectral feature and consequently also the conformational changes.

The visibility of the molecular feature depends on several factors. For most efficient coupling and therefore most prominent spectral splitting, the frequency of the molecular vibration and the plasmon resonance should be similar. On the other hand, the coupling strength is also influenced by the local near-field strength, which is known to be maximum slightly red-shifted with respect to the far-field scattering maximum, and thus, the antenna resonance should be slightly blue-detuned. Moreover, slight deviations in molecular coverage as well as a possibly varying quality factor of the array due to inhomogeneous broadening will influence the feature. All these factors come together and influence the visibility in our experiment. In order to choose dimensions with the best visibility, we varied the antenna length. For all lengths, qualitatively, the same results were obtained (see Figure S4 in the Supporting Information). Using a slit array with a length of $1.7 \mu\text{m}$, the amide I vibration is most pronounced being

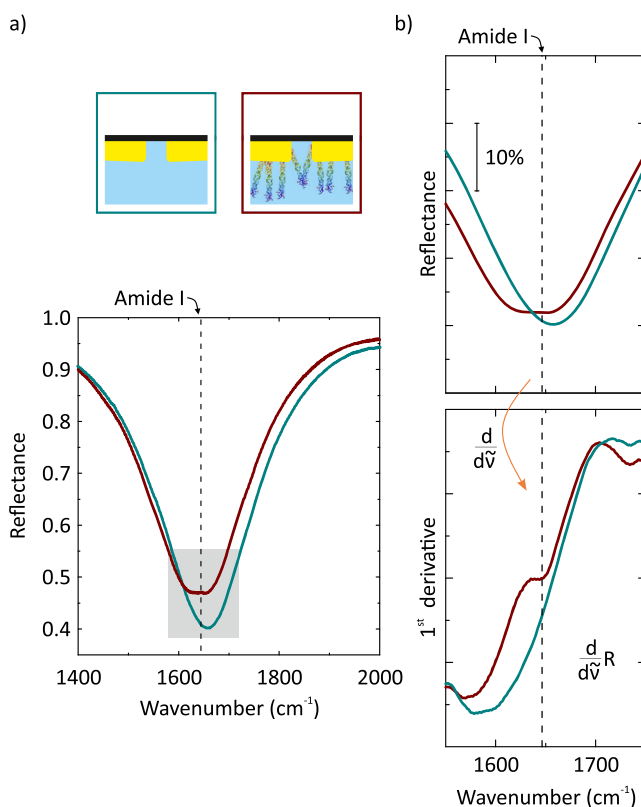


Figure 2. (a) Functionalization scheme. We cover the nanoslits with collagen peptides by immersing the sample into $5 \mu\text{M}$ D_2O -based solution of molecules for 24 h. We acquired the reflectance spectra before (dark green) and after (dark red) functionalization. The spectral position of the amide vibration is marked by the dashed line. (b) Zooming into the reflection spectrum (top panel), the spectral feature is difficult to see and in particular to track, and thus, the first derivative of the optical response is depicted (lower panel). The slope of the reflectance reveals that the amide vibration at 1644 cm^{-1} is specific for the functionalized nanostructures, whereas such signal is absent in the case of bare nanoslits.

located on a linear section of the first derivative and has therefore been chosen for the discussion in the main text. Additionally, we performed control experiments with collagen peptides self-assembled on a bare gold surface; please refer to Figure S5 in the Supporting Information.

Having nanoslits functionalized with collagen peptides, we continue with unfolding experiments of the prepared monolayer. Similar to many proteins, the folding behavior of collagen peptides is determined by the external environment. Therefore, we can switch the conformation of the molecule by changing the surroundings. It has been shown that heating of the collagen-peptide surroundings leads to structural transitions.^{46,49} On the other hand, sodium dodecyl sulfate (SDS) is also known to change protein secondary structure.^{50,51} At higher concentrations of SDS solution, the surfactant binds on the protein hydrophobic sites,⁵¹ which causes unfolding of the helices in collagen's triple helix. In other words, SDS causes the reversible denaturation of the biomolecules, similar to heating.

To examine if our nanosensor is able to detect a structural difference of the collagen-peptide monolayer, we induce the conformational changes with an SDS solution, which allows a direct transition from natural to denaturated states (Figure 3). The upper panel depicts the measured reflectance spectra, where the first derivative of optical response is shown on the

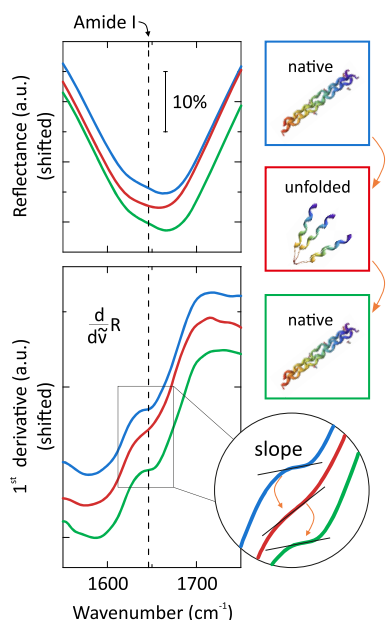


Figure 3. Changes in the secondary structure are induced by external chemical stimuli. The upper panel depicts reflectance spectra measured, whereas the lower one shows the first derivative of the optical response. The position of the characteristic vibrational feature of collagen-peptide 3x(PUG)₅ is shown as a dashed line. Utilizing a specially tailored flow cell, we immersed the sample into different surroundings in the following sequence: D₂O (blue), SDS solution (red), D₂O (green). Monitoring the slope change of the amide I spectral feature, we detect reversible structural changes of collagen peptides: from triple-helix to unfolded and back.

lower panel. The array of nanoslits being immersed in D₂O-based solution has the plasmonic resonance frequency close to the amide I vibration. As one can see at the lower panel, it is convenient to monitor the change of the slope at the frequency of amide vibration in order to track the changes of the secondary structure. Similar to Figure 2b, the characteristic vibrational feature of the molecules imprinted on the plasmonic resonance (dashed line) is visible. The three different measurements are color-coded here. We fill the flow cell with D₂O right after functionalization, which is now the initial state (blue curve). Next, we exchange the solution in the fluidic cell and by this add SDS impurity to the surrounding (red curve). The slope represents a weaker vibrational response of the molecules at amide I frequency. As mentioned above, such behavior was expected, because SDS causes denaturation of peptides. For collagen peptides, this starts by breaking the bonding between helices of the triple helix at first point. Therefore, there are less vibrations at the characteristic frequency, leading to a weaker spectral feature. The recipe of SDS solution we used was introduced previously in the literature.⁵² At the last step, we remove the chemical stimulus from the flow cell, which means replacement of SDS solution with D₂O (green curve). Consequently, it is clear that further solution exchange results in the triple-helical structure of collagen peptides and leads to a more pronounced spectral response. The same results are obtained for measurements performed for the slit arrays of different length (see Figure S6 in the Supporting Information).

The conformational transition from folded to unfolded states is the main focus in protein studies, and previous results show that our nanosensor is capable of such experiments.

Thus, to track the step-by-step transition of the collagen-peptide ensemble from the folded to the unfolded state, we utilize a thermal stimulus of structural changes (Figures S7–S9 in the Supporting Information). Therefore, we proceed with temperature-induced studies of the collagen-peptide monolayer (Figure 4). In the following studies, we measure the

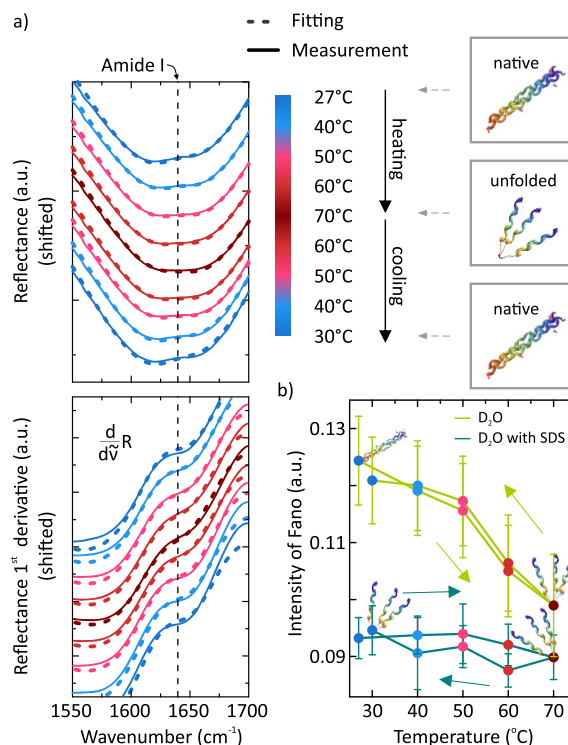


Figure 4. Monitoring thermally induced conformational changes of collagen peptides. (a) The frequency of amide vibration of molecules marked by a vertical dashed line; the temperature steps are color-coded. Solid lines depict the optical response at each temperature step. Reflectance spectra (upper panel) exhibit a spectral shift due to the temperature variation. However, the first derivative of the optical response (lower panel) reveals the change of the spectral feature at a frequency of amide vibration. Dashed curves show the results of fitting the experimental data by an analytical model, which shows excellent agreement with the measured optical response. (b) We extracted the intensity of molecular vibration by fitting a Fano profile to the measured spectra. After a temperature increase of the D₂O environment, the vibrational feature decreases in a sigmoidal manner (light green curve). However, in the control experiment, the SDS surrounding prevents this behavior (dark green curve), which is expected as molecules were denaturated at room temperature already.

spectra before heating, namely, at a temperature of 27 °C. Next, we heat the solution with the help of a PID controller up to 70 °C in steps of 10 °C. We perform reflection measurement at each temperature step. Similar to heating, we acquire the optical response at mentioned temperature steps during the cooling of the system. Therefore, we plot the spectra in a way that the measurement of the first temperature point is on top and the last at the bottom (Figure 4a).

As one can see from the reflectance spectra (Figure 4a, color-coded solid curves), the resonance frequency of the nanoslit array shifts with temperature, as the heating of the D₂O-based solution results in slight changes of the refractive index (see also Figure S11).⁵³ Similar to the previous experiment, the first derivative of the measured spectra

provides a more convenient way for monitoring folding of collagen peptides. As expected, the vibrational feature is weaker at higher temperatures. Despite this observation, we would like to investigate whether this phenomenon is due to conformational changes. As we know from literature and our reference measurements,⁴⁹ the intensity of collagen-peptide amide I vibration decreases with temperature and has reversible behavior. Furthermore, the strength of this molecular signal reveals the fraction of collagen folded.⁴⁹ Therefore, we extract the vibrational signal of molecules from our experimental data at each temperature step. To accomplish this idea, we perform fitting of the experimental data.

To describe the optical response analytically, we utilize a harmonic oscillator model. Namely, we assume that the plasmonic resonance around the resonance frequency is symmetric and thus has a Lorentzian profile. Also, because of the coupling of the molecules to the nanostructure, the vibrational feature of collagen peptide has a Fano profile.⁵⁴ However, due to the mismatch of the dipole moment between the molecular vibrations and plasmonic resonance of the nanoslits, the coupling is weak despite the good match of the resonant frequencies. Hence, the spectrum measured is the sum of both

$$\text{spectrum}(\omega) = L(\omega) + F(\omega)$$

where

$$L(\omega) = 1 - \frac{A}{\left(\frac{\omega - \omega_{\text{res}}}{\Gamma_{\text{res}}}\right)^2 + 1}$$

$$F(\omega) = \left[1 - \frac{\left(\frac{\omega - \omega_{\text{vib}}}{\Gamma_{\text{vib}}} + q\right)^2}{\left(\frac{\omega - \omega_{\text{vib}}}{\Gamma_{\text{vib}}}\right)^2 + 1} \right] \cdot I$$

There are a few characteristic constants: A is the modulation depth of plasmonic resonance, Γ_{res} is the full width at half-maximum of the plasmonic resonance, ω_{res} is the resonance frequency of nanostructure, ω_{vib} is the frequency of amide vibration, Γ_{vib} is the full width at half-maximum of amide vibration, and q is the asymmetry factor, which depends on the tuning ratio $\omega_{\text{vib}}/\omega_{\text{res}}$. We obtain the resonance frequency of the nanoslit array from the spectral centroid for each temperature.⁵⁵ In general, one would assume the asymmetry factor to be temperature-dependent, as the plasmon resonance is temperature-dependent due to a change of the effective refractive index with temperature. However, this shift is very small, which allows us to assume the asymmetry parameter of the Fano profile q to be constant. The validity of this assumption has been tested by assuming strongly varying asymmetry factors, which in fact show negligible influence on the results of the model (see Figure S10 in the Supporting Information). Thus, it can be obtained from fitting of the first spectrum (at 27 °C) and is used for all next fittings. The rest of the parameters mentioned are fixed and thus the same for all spectra (more details in the Supporting Information). Finally, there is one parameter left, namely, I , which is related to the intensity of molecular vibration.

Taking all mentioned points into account, we perform fitting of each experimental spectrum with a single open parameter in the vicinity of the nanoslit resonance (more in the Supporting Information, Figure S10). The analytically obtained spectra

demonstrate good agreement with our experimental results (Figure 4a, color-coded dash curves). As we introduced this model in order to extract the molecular vibration from the experimental data, we normalize the analytically obtained amide vibration to the antenna profile and plot the resulting signal versus temperature (Figure 4b, light green). This delivers a scalar value that describes the strength of the vibrational signal. The results depicted in Figure 4 demonstrate a reversible conformational change of the collagen-peptide monolayer under external stimuli. Similar to the bulk solutions, heating the D₂O surroundings of the molecules adsorbed on the gold surface induces structural changes in expected fashion.

As a control experiment, we performed the same temperature-induced measurements and data analysis for SDS-based surroundings (Figure S11 in the Supporting Information), where we expected the molecules to be denaturated from the beginning, and thus, additional heating should have no effect (Figure 4b, dark green). As expected, the SDS environment denaturates the peptides, and in combination with heating, there are no structural changes visible. Similar behavior was detected for the slits with different lengths (Figure S12 in the Supporting Information).

Thus, our measurements and analytical analysis clearly validate our approach of in vitro monitoring of structural changes of collagen molecules at low concentrations utilizing resonant surface-enhanced infrared spectroscopy with plasmonic nanoslits. Our concept allows for the observation of conformational changes under different stimuli, including temperature change, and detailed analytical analysis reveals the conformational transition from one secondary structure to another.

CONCLUSIONS

To summarize, we experimentally demonstrated the unique capabilities for ultrasensitive in vitro detection of the triple-helical structure of collagen-like molecules at the monolayer scale utilizing mid-IR resonant plasmonic nanoslits as a sensing platform. As a result of the higher average SEIRA signal of the inverse nanostructure in comparison to nanoantennas,⁴⁵ nanoslits are well suited for structural detections of minicollagens as well as other proteins. Our biosensor enables reliable tracking of collagen conformational changes under various external stimuli via monitoring the amide I vibration. The analysis of our experimental data with a simple analytical model also reveals the expected folding behavior. Our plasmonic-based nanosensor is promising for mid-IR secondary structural analysis on minute protein samples including transient species in dynamic conformational processes, which might bring more degrees of freedom to applications in medical diagnosis.

ASSOCIATED CONTENT

Supporting Information

The Supporting Information is available free of charge on the ACS Publications website at DOI: 10.1021/acssensors.9b00377.

Figures of fluidic cells used for the in vitro measurements, details regarding FTIR measurements and functionalization procedures, reference IR and CD measurements, results of collagen folding for different antenna lengths, details concerning data analysis (PDF)

AUTHOR INFORMATION

Corresponding Author

*E-mail: neubrech@kip.uni-heidelberg.de. (F.N.)

ORCID

Rostyslav Semenyshyn: 0000-0001-6818-7500

Christian Huck: 0000-0003-3012-3901

Frank Neubrech: 0000-0002-5437-4118

Notes

The authors declare no competing financial interest.

ACKNOWLEDGMENTS

We thank Prof. Armin Geyer (University of Marburg) for stimulating the use of this system for folding analysis. Also, we thank Dr. Christoph Stanglmair, who contributed to a discussion regarding the control experiments. The authors gratefully acknowledge financial support by the ERC Advanced Grant (COMPLEXPLAS), Deutsche Forschungsgemeinschaft (SPP1839), Baden-Württemberg Stiftung (PROTEINSENS), MWK Baden-Württemberg (IQST, ZAQuant), and BMBF (03IS2101E).

REFERENCES

- (1) Pauling, L.; Corey, R. B.; Branson, H. R. The structure of proteins: Two hydrogen-bonded helical configurations of the polypeptide chain. *Proc. Natl. Acad. Sci. U. S. A.* **1951**, *37*, 205–211.
- (2) Clore, G. M.; Gronenborn, A. M. Structures of larger proteins in solution: three- and four-dimensional heteronuclear NMR spectroscopy. *Science* **1991**, *252*, 1390–1399.
- (3) Sanger, F. The Arrangement of Amino Acids in Proteins. *Adv. Protein Chem.* **1952**, *7*, 1–67.
- (4) Anfinsen, C. B. The formation and stabilization of protein structure. *Biochem. J.* **1972**, *128*, 737–749.
- (5) Govindarajan, S.; Recabarren, R.; Goldstein, R. A. Estimating the total number of protein folds. *Proteins: Struct., Funct., Genet.* **1999**, *35*, 408–414.
- (6) Soto, C.; Estrada, L.; Castilla, J. Amyloids, prions and the inherent infectious nature of misfolded protein aggregates. *Trends Biochem. Sci.* **2006**, *31*, 150–155.
- (7) Knowles, T. P. J.; Vendruscolo, M.; Dobson, C. M. The amyloid state and its association with protein misfolding diseases. *Nat. Rev. Mol. Cell Biol.* **2014**, *15*, 384–396.
- (8) Kelly, S. M.; Jess, T. J.; Price, N. C. How to study proteins by circular dichroism. *Biochim. Biophys. Acta, Proteins Proteomics* **2005**, *1751*, 119–139.
- (9) Greenfield, N. J. Using circular dichroism spectra to estimate protein secondary structure. *Nat. Protoc.* **2006**, *1*, 2876–2890.
- (10) Wüthrich, K. Protein structure determination in solution by NMR spectroscopy. *J. Biol. Chem.* **1990**, *265*, 22059–22062.
- (11) Aslam, N.; Pfender, M.; Neumann, P.; Reuter, R.; Zappe, A.; Fávoro de Oliveira, F.; Denisenko, A.; Sumiya, H.; Onoda, S.; Isoya, J.; Wrachtrup, J. Nanoscale nuclear magnetic resonance with chemical resolution. *Science* **2017**, *357*, 67–71.
- (12) Boutet, S.; Lomb, L.; Williams, G. J.; Barends, T. R. M.; Aquila, A.; Doak, R. B.; Weierstall, U.; DePonte, D. P.; Steinbrener, J.; Shoeman, R. L.; et al. High-Resolution Protein Structure Determination by Serial Femtosecond Crystallography. *Science* **2012**, *337*, 362–364.
- (13) Schotte, F.; Lim, M.; Jackson, T. A.; Smirnov, A. V.; Soman, J.; Olson, J. S.; Phillips, G. N. J.; Wulff, M.; Anfinrud, P. A. Watching a protein as it functions with 150-ps time-resolved x-ray crystallography. *Science* **2003**, *300*, 1944–1947.
- (14) Ruggeri, F. S.; Adamcik, J.; Jeong, J. S.; Lashuel, H. A.; Mezzenga, R.; Dietler, G. Influence of the β -sheet content on the mechanical properties of aggregates during amyloid fibrillization. *Angew. Chem., Int. Ed.* **2015**, *54*, 2462–2466.
- (15) Amenabar, I.; Poly, S.; Nuansing, W.; Hubrich, E. H.; Govyadinov, A. A.; Huth, F.; Krutokhvostov, R.; Zhang, L.; Knez, M.; Heberle, J. Structural analysis and mapping of individual protein complexes by infrared nanospectroscopy. *Nat. Commun.* **2013**, *4*, 2890.
- (16) Barth, A. Infrared spectroscopy of proteins. *Biochim. Biophys. Acta, Bioenerg.* **2007**, *1767*, 1073–1101.
- (17) Lippert, J. L.; Tyminski, D.; Desmeules, P. J. Determination of the secondary structure of proteins by laser Raman spectroscopy. *J. Am. Chem. Soc.* **1976**, *98*, 7075–7080.
- (18) Barth, A.; Haris, P. I. *Biological and biomedical infrared spectroscopy*; IOS Press, 2009.
- (19) Dousseau, F.; Pézolet, M. Determination of the secondary structure content of proteins in aqueous solutions from their amide I and amide II infrared bands. Comparison between classical and partial least-squares methods. *Biochemistry* **1990**, *29*, 8771–8779.
- (20) Venyaminov, S. Y.; Kalnin, N. N. Quantitative IR spectrophotometry of peptide compounds in water (H₂O) solutions. II. Amide absorption bands of polypeptides and fibrous proteins in α -, β -, and random coil conformations. *Biopolymers* **1990**, *30*, 1259–1271.
- (21) Dzwolak, W.; Smirnovas, V. A conformational α -helix to β -sheet transition accompanies racemic self-assembly of polylysine: An FT-IR spectroscopic study. *Biophys. Chem.* **2005**, *115*, 49–54.
- (22) Dzwolak, W.; Muraki, T.; Kato, M.; Taniguchi, Y. Chain-length dependence of α -helix to β -sheet transition in polylysine: Model of protein aggregation studied by temperature-tuned FTIR spectroscopy. *Biopolymers* **2004**, *73*, 463–469.
- (23) Deflores, L. P.; Ganim, Z.; Nicodemus, R. A.; Tokmakoff, A. Amide I-II 2D IR spectroscopy provides enhanced protein secondary structural sensitivity. *J. Am. Chem. Soc.* **2009**, *131*, 3385–3391.
- (24) Neubrech, F.; Pucci, A.; Cornelius, T. W.; Karim, S.; García-Exarri, A.; Aizpurua, J. Resonant plasmonic and vibrational coupling in a tailored nanoantenna for infrared detection. *Phys. Rev. Lett.* **2008**, *101*, 157403.
- (25) Kühner, L.; Hentschel, M.; Zschieschang, U.; Klauk, H.; Vogt, J.; Huck, C.; Giessen, H.; Neubrech, F. Nanoantenna-Enhanced Infrared Spectroscopic Chemical Imaging. *ACS Sens* **2017**, *2*, 655–662.
- (26) Neubrech, F.; Huck, C.; Weber, K.; Pucci, A.; Giessen, H. Surface-Enhanced Infrared Spectroscopy Using Resonant Nanoantennas. *Chem. Rev.* **2017**, *117*, 5110–5145.
- (27) Cerjan, B.; Yang, X.; Nordlander, P.; Halas, N. J. Asymmetric Aluminum Antennas for Self-Calibrating Surface-Enhanced Infrared Absorption Spectroscopy. *ACS Photonics* **2016**, *3*, 354–360.
- (28) Huck, C.; Neubrech, F.; Vogt, J.; Toma, A.; Gerbert, D.; Katzmann, J.; Härtling, T.; Pucci, A. Surface-enhanced infrared spectroscopy using nanometer-sized gaps. *ACS Nano* **2014**, *8*, 4908–4914.
- (29) Brown, L. V.; Yang, X.; Zhao, K.; Zheng, B. Y.; Nordlander, P.; Halas, N. J. Fan-shaped gold nanoantennas above reflective substrates for surface-enhanced infrared absorption (SEIRA). *Nano Lett.* **2015**, *15*, 1272–1280.
- (30) Wang, T.; Nguyen, V. H.; Buchenauer, A.; Schnakenberg, U.; Taubner, T. Surface enhanced infrared spectroscopy with gold strip gratings. *Opt. Express* **2013**, *21*, 9005–9010.
- (31) Wu, C.; Khanikaev, A. B.; Adato, R.; Arju, N.; Yanik, A. A.; Altug, H.; Shvets, G. Fano-resonant asymmetric metamaterials for ultrasensitive spectroscopy and identification of molecular monolayers. *Nat. Mater.* **2012**, *11*, 69–75.
- (32) Becker, J.; Trügler, A.; Jakab, A.; Hohenester, U.; Sönnichsen, C. The optimal aspect ratio of gold nanorods for plasmonic biosensing. *Plasmonics* **2010**, *5*, 161–167.
- (33) Zhang, Y.; Zhen, Y.-R.; Neumann, O.; Day, J. K.; Nordlander, P.; Halas, N. J. Coherent anti-Stokes Raman scattering with single-molecule sensitivity using a plasmonic Fano resonance. *Nat. Commun.* **2014**, *5*, 4424.
- (34) Adato, R.; Yanik, A. A.; Amsden, J. J.; Kaplan, D. L.; Omenetto, F. G.; Hong, M. K.; Erramilli, S.; Altug, H. Ultra-sensitive vibrational

spectroscopy of protein monolayers with plasmonic nanoantenna arrays. *Proc. Natl. Acad. Sci. U. S. A.* **2009**, *106*, 19227–19232.

(35) Anker, J. N.; Hall, W. P.; Lyandres, O.; Shah, N. C.; Zhao, J.; Van Duyne, R. P. Biosensing with plasmonic nanostructure. *Nat. Mater.* **2008**, *7*, 442–453.

(36) Rodrigo, D.; Limaj, O.; Janner, D.; Etezadi, D.; García De Abajo, F. J.; Pruneri, V.; Altug, H. Mid-Infrared Plasmonic Biosensing with Graphene. *Science* **2015**, *349*, 165–168.

(37) Ament, I.; Prasad, J.; Henkel, A.; Schmachtel, S.; Sönnichsen, C. Single unlabeled protein detection on individual plasmonic nanoparticles. *Nano Lett.* **2012**, *12*, 1092–1095.

(38) Adato, R.; Altug, H. In-situ ultra-sensitive infrared absorption spectroscopy of biomolecule interactions in real time with plasmonic nanoantennas. *Nat. Commun.* **2013**, *4*, 2154.

(39) Limaj, O.; Etezadi, D.; Wittenberg, N. J.; Rodrigo, D.; Yoo, D.; Oh, S. H.; Altug, H. Infrared Plasmonic Biosensor for Real-Time and Label-Free Monitoring of Lipid Membranes. *Nano Lett.* **2016**, *16*, 1502–1508.

(40) Etezadi, D.; Warner, J. B.; Ruggeri, F. S.; Dietler, G.; Lashuel, H. A.; Altug, H. Nanoplasmonic mid-infrared biosensor for in vitro protein secondary structure detection. *Light: Sci. Appl.* **2017**, *6*, No. e17029.

(41) Semenishyn, R.; Hentschel, M.; Stanglmair, C.; Teutsch, T.; Tarin, C.; Pacholski, C.; Giessen, H.; Neubrech, F. Vitro Monitoring Conformational Changes of Polypeptide Monolayers Using Infrared Plasmonic Nanoantennas. *Nano Lett.* **2019**, *19*, 1–7.

(42) Etezadi, D.; Warner, J. B.; Lashuel, H. A.; Altug, H. Real-Time In Situ Secondary Structure Analysis of Protein Monolayer with Mid-Infrared Plasmonic Nanoantennas. *ACS Sensors* **2018**, *3*, 1109–1117.

(43) Hentschel, M.; Weiss, T.; Bagheri, S.; Giessen, H. Babinet to the Half: Coupling of Solid and Inverse Plasmonic Structures. *Nano Lett.* **2013**, *13*, 4428–4433.

(44) Ögüt, B.; Vogelgesang, R.; Sigle, W.; Talebi, N.; Koch, C. T.; van Aken, P. A. Hybridized Metal Slit Eigenmodes as an Illustration of Babinet's Principle. *ACS Nano* **2011**, *5*, 6701–6706.

(45) Huck, C.; Vogt, J.; Sendner, M.; Hengstler, D.; Neubrech, F.; Pucci, A. Plasmonic Enhancement of Infrared Vibrational Signals: Nanoslits versus Nanorods. *ACS Photonics* **2015**, *2*, 1489–1497.

(46) Weiher, F.; Schatz, M.; Steinem, C.; Geyer, A. Silica precipitation by synthetic minicollagens. *Biomacromolecules* **2013**, *14*, 683–687.

(47) Park, S.; Klein, T. E.; Pande, V. S. Folding and Misfolding of the Collagen Triple Helix: Markov Analysis of Molecular Dynamics Simulations. *Biophys. J.* **2007**, *93*, 4108–4115.

(48) Fallah, M. A.; Stanglmair, C.; Pacholski, C.; Hauser, K. Devising self-assembled-monolayers for surface-enhanced infrared spectroscopy of pH-driven poly-l-lysine conformational changes. *Langmuir* **2016**, *32*, 7356–7364.

(49) Bryan, M. A.; Brauner, J. W.; Anderle, G.; Flach, C. R.; Brodsky, B.; Mendelsohn, R. FTIR studies of collagen model peptides: Complementary experimental and simulation approaches to conformation and unfolding. *J. Am. Chem. Soc.* **2007**, *129*, 7877–7884.

(50) Gopal, R.; Park, J. S.; Seo, C. H.; Park, Y. Applications of circular dichroism for structural analysis of gelatin and antimicrobial peptides. *Int. J. Mol. Sci.* **2012**, *13*, 3229–3244.

(51) Xu, Q.; Keiderling, T. A. Effect of sodium dodecyl sulfate on folding and thermal stability of acid-denatured cytochrome c: A spectroscopic approach. *Protein Sci.* **2004**, *13*, 2949–2959.

(52) Wang, Y.; Chang, Y. C. Synthesis and conformational transition of surface-tethered polypeptide: Poly(L-lysine). *Macromolecules* **2003**, *36*, 6511–6518.

(53) Hale, G. M.; Querry, M. R.; Rusk, A. N.; Williams, D. Influence of temperature on the spectrum of water. *J. Opt. Soc. Am.* **1972**, *62*, 1103–1108.

(54) Giannini, V.; Francescato, Y.; Amrania, H.; Phillips, C. C.; Maier, S. A. Fano resonances in nanoscale plasmonic systems: A parameter-free modeling approach. *Nano Lett.* **2011**, *11*, 2835–2840.

(55) Dahlin, A. B.; Tegenfeldt, J. O.; Höök, F. Improving the Instrumental Resolution of Sensors Based on Localized Surface Plasmon Resonance. *Anal. Chem.* **2006**, *78*, 4416–4423.